CORTEX 132 (2020) 281–295

Available online at www.sciencedirect.com

ScienceDirect

Journal homepage: www.elsevier.com/locate/cortex

Research Report

A robust neural familiar face recognition response in a dynamic (periodic) stream of unfamiliar faces

Xiaoqian Yan [a,b] *and Bruno Rossion* [a,b,c,*]

[a] *Université de Lorraine, CNRS, CRAN, Nancy, France*
[b] *Institute of Research in Psychological Science, Institute of Neuroscience, Université Catholique de Louvain, Louvain-La-Neuve, Belgium*
[c] *Université de Lorraine, CHRU-Nancy, Service de Neurologie, Nancy, France*

ARTICLE INFO

Article history:
Received 28 March 2020
Reviewed 11 June 2020
Revised 22 July 2020
Accepted 10 August 2020
Action editor Holger Wiese
Published online 8 September 2020

Keywords:
Familiar face recognition
Frequency-tagging
Inversion
EEG

ABSTRACT

We present an objective and sensitive approach to measure human familiar face recognition (FFR) across variable facial identities. Twenty-six participants viewed sequences of natural images of different unfamiliar faces presented at a fixed rate of 6 Hz (i.e., 6 faces by second), with variable natural images of different famous face identities appearing periodically every 7th image (i.e., .86 Hz). Participants were unaware of the goal of the study and performed an orthogonal task. Following only seven minutes of visual stimulation, the FFR response was objectively identified in the EEG spectrum at .86 Hz and its harmonics (1.71 Hz, etc.) over bilateral occipito-temporal regions, being significant in every individual participant. When the exact same images appeared upside-down, the FFR response amplitude reduced by more than 80%, and was uncorrelated across individuals to the upright face response. The FFR for upright faces emerges between 160 and 200 msec following the famous face onset over bilateral occipito-temporal region and lasts until about 560 msec. The stimulation paradigm offers an unprecedented way to characterize rapid and automatic human face familiarity recognition across individuals, during development and clinical conditions, also providing original information about the time-course and neural basis of human FFR in temporally constrained stimulation conditions with natural images.

* *Corresponding author*. CRAN UMR 7039, CNRS - Universite de Lorraine, 2 Avenue de la forêt de Haye, 54516, Vandoeuvre-lès-Nancy, France.
E-mail address: bruno.rossion@univ-lorraine.fr (B. Rossion).
https://doi.org/10.1016/j.cortex.2020.08.016

1. Introduction

Humans living in modern societies are constantly surrounded by faces in their physical environment or through the media, with only a fraction of these faces being familiar, i.e. previously encoded in memory. Accurately and rapidly differentiating familiar from unfamiliar faces, even before accessing specific semantic, affective or verbal information associated to a given identity, constitutes therefore one of the most frequent, socially important, functions of the human brain. Yet, this familiar face recognition (FFR) function is also extremely challenging, for two main reasons. First, because individual (familiar and unfamiliar) faces look alike (i.e., they share a common configuration of the same kinds of facial features), requiring fine-grained visual processes to discriminate them; and second because the same face identity, irrespective of its long term familiarity, can change drastically from one view to another (within person identity variation; Jenkins, White, Van Montfort, & Burton, 2011; Burton, Kramer, Ritchie, & Jenkins, 2016).

Since the seminal study of Bruce (1982), and particularly over the last two decades, a large body of research has emphasized the strong difference between familiar and unfamiliar faces in terms of the ability to generalize across viewing conditions (i.e., changes in head orientation, lighting conditions, etc.). It is widely acknowledged that matching different views of the same face identity, with or without delay between pictures, is achieved much better for familiar than unfamiliar faces (Burton, Bruce, & Hancock, 1999; Bruce, 1982; Bruce, Henderson, Newman, & Burton, 2001; Megreya & Burton, 2006; Young & Burton, 2018; see Hancock, Bruce, & Burton, 2000, and Johnston & Edmonds, 2009 for reviews). The outcome of these studies is generally taken as evidence for different representations/processes between familiar and unfamiliar faces (e.g., Megreya & Burton, 2006; Young & Burton, 2018). Yet, the nature of these differential representations and processes remains unknown. For instance, a key issue is whether these differences arise at the level of visual (i.e., unimodal) representations/processes, or if they essentially reflect the rich associations of familiar faces only with semantic/verbal and affective representations (Bruce, 1982; Rossion, 2018; Schwartz & Yovel, 2016). To clarify this issue, researchers may turn to neural measures of differences between familiar and unfamiliar faces.

Neurofunctional models of familiar face recognition have proposed that successful recognition of familiar faces involves a rich and distributed network in the human brain, including face-selective regions of the visual cortex and other more general regions in the anterior and medial temporal lobe linked to the retrieval of biographical information, names and emotional responses attached to the familiar faces (Gobbini & Haxby, 2007; Natu & O'Toole, 2011). However, clear differential neural activation patterns to familiar (including famous celebrity faces, personal familiar faces, and experimentally learned faces) and unfamiliar faces are rare and rather inconsistent in terms of localization, direction and amplitude of effects across human neuroimaging studies. On the one hand, the lack of systematic differences between familiar and unfamiliar faces in anterior temporal lobe regions could largely be due to the significant drop in signal-to-noise ratio (SNR) due to magnetic susceptibility artifacts in these regions (Axelrod & Yovel, 2013; Wandell, 2011; see Fig. 1 in Rossion, Jacques, & Jonas, 2018). On the other hand, differences between familiar and unfamiliar faces in posterior face-selective regions of the ventral occipito-temporal cortex (VOTC), thought to underlie visual face processes, have been largely inconsistent. In some studies, familiar faces evoke a larger response in these regions (e.g., Gobbini, Leibenluft, Santiago, & Haxby, 2004; Pierce, Haist, Sedaghat, & Courchesne, 2004), in other studies a smaller response is found for familiar faces (e.g., Rossion, Schiltz, & Crommelinck, 2003), with no differences in others (e.g., Gorno-Tempini & Price, 2001; Leveroni et al., 2000). The discrepancies between studies at the level of these brain regions could be due to different tasks used in the various studies, with an explicit task (e.g., to discriminate familiar from unfamiliar faces) usually eliciting a larger response to familiar faces (e.g., Henson, Shallice, Gorno-Tempini, & Dolan, 2002; Sergent, Ohta, & MacDonald, 1992). Yet, explicit tasks could also introduce the contribution of many other factors beyond visual face processes, such as task understanding, motivation, or decisional processes. Moreover, while face-related tasks might increase absolute neural response amplitude, it may also reduce response specificity by recruiting additional cortical regions (Yan, Liu-Shuang, & Rossion, 2019).

Differences between familiar and unfamiliar faces have also, and mainly, been investigated with electroencephalography (EEG), typically using a standard visual stimulation approach in which stimuli presented at a slow and non-periodic rate elicit time-locked changes in EEG responses, i.e. event-related potentials (ERPs). Numerous EEG studies have compared the amplitude and latency of the N170 component – the earliest and main face-selective ERP, peaking over occipito-temporal sites at about 170 msec (Bentin, Allison, Puce, Perez, & McCarthy, 1996; Rossion & Jacques, 2011 for review) - to pictures of familiar and unfamiliar faces. A number of studies have failed to show any N170 difference for familiar and unfamiliar faces (e.g., Begleiter, Porjesz, & Wang, 1995; Gosling & Eimer, 2011; Pierce et al., 2011; Rossion et al., 1999; Tanaka, Curran, Porterfield, & Collins, 2006). Yet, a small face familiarity effect has also been reported in some studies, with larger (e.g., Barragan-Jason, Cauchoix, & Barbeau, 2015; Caharel, Courtay, Bernard, Lalonde, & Rebaï, 2005, 2002; Jemel, Schuller, & Goffaux, 2010; Wild-Wall, Dimigen, & Sommer, 2008) or smaller (e.g. Huang et al., 2017; Jemel, Pisani, Calabria, Crommelinck, & Bruyer, 2003; Todd, Lewis, Meusel, & Zelazo, 2008) amplitudes to familiar relative to unfamiliar faces. Inconsistent results have also been reported on the corresponding M170 component evoked in magnetoencephalography (MEG) studies (e.g., Ewbank & Andrews, 2008; Kloth et al., 2006). The inconsistencies of N170/M170 differences to familiar and unfamiliar faces could be due to many factors such as the type of familiar face studied (own face, personally familiar faces, celebrity, or lab learned faces), the number of times a face stimulus is presented throughout the experiment, the task (e.g., passive viewing, face gender discrimination, facial expression judgment, or face familiarity judgment), and so on.

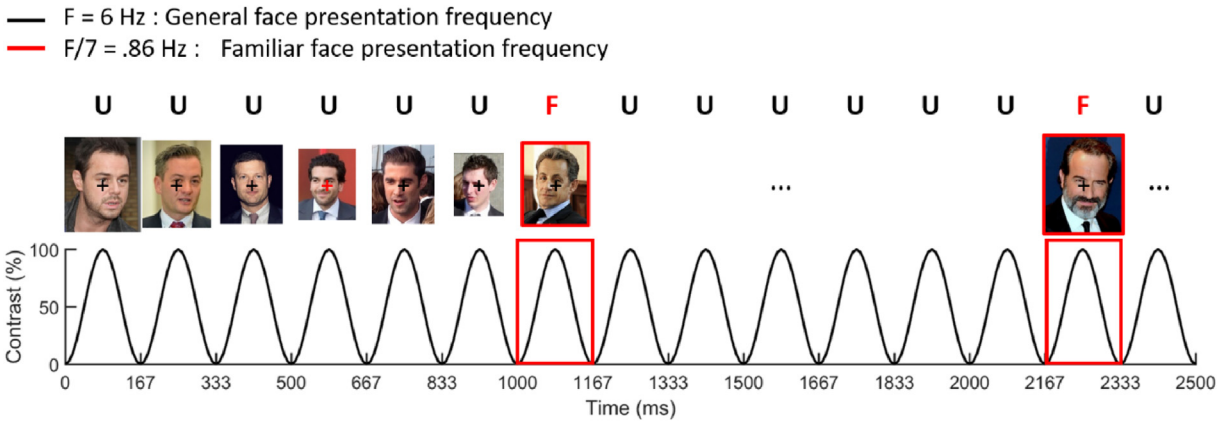

Fig. 1 – Schematic illustration of the experimental design. Different images of unfamiliar faces (U) are presented through sinusoidal contrast modulation at a fixed rate of 6 Hz (i.e., 6 images by second), with different familiar faces (F) embedded at every 7th image (i.e., 6/7 Hz). The two familiar celebrity faces (F) shown in the figure here are Nicolas Sarkozy and Jean Dujardin. On any given sequence of 74 sec (including 2 sec fade-in and fade-out), participants had to detect the color change of a central fixation cross (from black to red, during 200 msec) and respond as soon and as accurately as possible (there were 6 target responses). Face images shown here are with license permits, however, for unfamiliar face identities, only the third face identity was used in the current experiment. For license information, Danny Dyer, Jean Dujardin, and Elyas M'Barek: Pictures licensed under the Creative Commons Attribution-Shared Alike 3.0 Unported. Attribution: Hilton 1949, Georges Biard, and Manfred Werner, respectively. Robert Biedroń: Pictures licensed under the Creative Commons Attribution-Shared Alike 3.0 Poland. Attribution: Adrian Grycuk. Dermot Oleary: Pictures under the Creative Commons Attribution-Shared Alike 4.0 International. Attribution: Walterlan Papettti. Blake Harrison, Matt Johnson, and Nicolas Sarkozy: Pictures under the Creative Commons Attribution 2.0 Generic. Attribution: Damo 1977, Robert Clarke, and European People's Party, respectively.

A more consistent face familiarity effect has been reported at about 200–350 msec post-stimulus onset over the inferior occipito-temporal region, showing an enhanced negativity for both famous faces (e.g., Barragan-Jason et al., 2015; Gosling & Eimer, 2011; Jemel et al., 2010; Wiese et al., 2019), personally familiar faces (Caharel et al., 2007), and newly learned faces (Rossion et al., 1999; Tanaka et al., 2006). A larger repetition effect ("N250r") for familiar than unfamiliar faces has also been described in this time-range (e.g., Begleiter et al., 1995; Pierce et al., 2011; Schweinberger, Pickering, Jentzsch, Burton, & Kaufmann, 2002, 2004).

Besides these effects, ERPs to familiar faces are typically reflected by increased negative potentials maximal around 400 msec (e.g., Bentin & Deouell, 2000; Eimer, 2000; Jemel, Pisani, Rousselle, Crommelinck, & Bruyer, 2005). A later enhanced positivity to familiar faces peaking at about 600 msec has also been reported in some studies (e.g., Bentin & Deouell, 2000; Eimer, 2000; Gosling & Eimer, 2011; Wiese et al., 2019). Usually, these later negative and positive components are much more broadly distributed across anterior, central parietal, and posterior regions, compared to the earlier components.

Overall, while these studies provide useful (albeit often contradictory) information about the time-course of FFR, the distribution of these effects on different time-domain components, with different polarities and scalp topographies, make it virtually impossible to rapidly derive a sensitive and objective compact measure of FFR in a group of individuals, let alone at the individual participant level. This makes it difficult to address key issues regarding the nature of the FFR function in humans, i.e. how it is affected by various physical (e.g., size, contrast, spatial frequency content, head orientation, lighting conditions, etc.) and semantic (i.e., knowledge about familiar identities) parameters. Moreover, besides robust familiarity ERP effects observed recently for natural images of personally familiar faces but not famous faces (Wiese et al., 2019), sensitivity at the individual level has not been demonstrated, preventing the reliable use of these measures to characterize impairments at FFR in single individuals, including neurological and neuropsychiatric patients. What would be desirable to address these issues is an objectively identifiable and readily quantifiable sensitive FFR measure. Ideally, this measure should be implicit, relating to the automaticity of FFR, and reflect the rapid speed at which this function is achieved by the human brain. Taking advantage of the EEG frequency-tagging approach, in which stimulus-related responses are expressed in the frequency-domain following relatively fast periodic visual stimulation (Regan, 1966; see Norcia, Appelbaum, Ales, Cottereau, & Rossion, 2015 for review), a recent study proposed such a robust and sensitive approach to measure familiar face *identity* recognition with natural images (Zimmermann, Yan, & Rossion, 2019). In this latter study, different natural face images of a *single* famous celebrity were embedded periodically (at every 7th image, .86 Hz) among different unfamiliar images presented at a fixed rate of 6 Hz (i.e., 6 images by second).

Following a few minutes of stimulation only, a neural recognition response recorded with EEG at the predefined frequency of .86 Hz and harmonics were detected over bilateral occipito-temporal region. A subsequent study showed that the neural response obtained in these conditions is reduced substantially (i.e., by a factor of 6) in a group of participants who did not know the familiar target faces (Yan, Zimmermann, & Rossion, 2020; see also, Campbell, Louw, Michniak, & Tanaka, 2020).

Here, our goal is to capitalize on these findings to extend this type of response to *different* familiar facial identities, i.e., measuring a *generic* FFR neural response. This was tested in the present study by presenting *different* celebrity faces (with highly variable views) periodically (i.e., every 7th image) among different unfamiliar faces during each stimulation sequence (Fig. 1). An obvious interest of this generic FFR measure is that it cannot be tied to specific physical features of a familiar face identity. Nevertheless, stimulation sequences with the same images of faces presented upside-down were also presented in order to isolate and quantify FFR effects that cannot be due to physical differences between familiar and unfamiliar face images. Moreover, by increasing the temporal distance between the familiar faces from unfamiliar faces in the stimulation sequences (i.e., every 7th stimuli or .86 Hz, every 1167 msec) as compared to previous studies, the time-course of the FFR response was explored and compared to standard ERP studies as reviewed above.

2. Methods

2.1. Participants

Twenty-seven Caucasian individuals, mainly undergraduate students from the Université Catholique de Louvain, participated in the experiment in total. Sixteen participants completed a first version of the experiment, and 11 participants completed a slightly modified version of the experiment (see below, section 'Stimuli') a few months later. Among these 11 participants, one of them also participated in the first version of the experiment. We removed data of one individual from the first version of the experiment after testing because of too much noise/muscular artefacts in the EEG data. There was no age difference between the two groups of participants, $t_{(24)} = .75$, $p > .1$. The final sample consisted of 26 participants (10 males; mean age, 22 ± 2.13 years). All participants were right-handed by self-report and had normal or corrected-to-normal vision. None had reported to have a history of neurological or psychiatric disorder. All participants gave their written consent prior to the experiment. The Biomedical Ethical committee of University of Louvain (ref no. B403201111965) approved the study.

2.2. Stimuli

In the first version of the experiment, stimuli consisted of 240 color images of famous male celebrity faces (12 different face identities each with 20 different natural images). Six famous French celebrities served as familiar faces: *actors Dany Boon and Jean Dujardin, television presenters Cyril Hanouna and Nagui Fam (Nagui), former French president Nicolas Sarkozy, and singer Pierre Garand (Garou)*. These six celebrities were selected based on pilot questionnaires among a sample of participants from other experiments, identifying the most famous face identities among the young adult of the French-speaking population of Belgium. Another six random French and British celebrities served as unfamiliar faces in the experiment. Faces varied greatly in head orientation, lighting, expression, etc. Visual properties of the images from two stimuli sets were considered and matched concerning age, hair color, and face appearances, to avoid potential image distinctiveness from one set than the other. Image size was 200 × 250 pixels, which extended a visual angle of approximately 8.5° in width and 9.1° in height viewing from 80 cm away.

In version 1 of the experiment, the number of facial identities (i.e., 6) is strictly matched between familiar and unfamiliar faces, with each identity being presented across 20 variable images. However, since the number of unfamiliar face presentations is 6 times larger than the number of familiar face presentation (see Fig. 1), each unfamiliar face identity is, on average, shown 6 times more than each familiar face identity in the experiment. Therefore, to ensure that this difference in presentation frequency does not account for the FFR response, we ran a second version of the experiment, which included another 30 unfamiliar faces. In this second version, there were a total of 36 unfamiliar face identities to strictly balance the face identity *repetitions* of familiar and unfamiliar faces (but not the number of identities). Thus, each face identity was presented 10 times (with 10 different natural images) during each stimulation sequence of 70 sec. All the other parameters of the stimuli were identical to experiment version one.

Overall, 23 out of 26 participants reported to know all six familiar identities very well. Two participants reported to have heard of *Garou*, but could not visualize his face, nor did they know his profession. One participant recognized the face of *Cyril Hanouna*, but had no idea of his name or profession. However, our analysis showed that all the three participants showed significant and equivalent FFR responses compared to the rest of the participants. In addition, several participants reported to know *Christophe Michalak* (5 individuals) and *Marc Levy* (5 individuals) used in the unfamiliar face set, but they reported to have barely seen them from social media (e.g., TV, newspaper, etc.), and none of them could visualize their faces.

2.3. Procedure

2.3.1. EEG testing

In each stimulation sequence, unfamiliar faces were presented at a fixed rate of 6 Hz over 74 sec (including 2 sec stimuli fade-in and 2 sec fade-out), selected randomly by the stimulation program, avoiding that the exact same image appeared consecutively. A familiar face image was inserted every 7th image (i.e., 6/7 Hz, .86 Hz, Fig. 1). Critically, and in contrast to previous studies (Campbell et al., 2020; Yan et al., 2020; Zimmerman et al., 2019) the familiar images within a sequence were of different face identities. The EEG responses elicited at 6 Hz and its harmonics reflects a general visual response to all face stimuli against a uniform grey background, a mixture of low- (e.g., luminance, contrast changes)

and high-level (e.g., face-related) visual responses. Most importantly, responses at .86 Hz and its harmonics should reflect a FFR response independently of the physical attributes of a specific identity. All face stimuli were presented through sinewave modulation of contrast, as in most studies using this approach (e.g., Liu-Shuang, Norcia, & Rossion, 2014; Retter & Rossion, 2016; Zimmermann et al., 2019), making a smooth transition between images. At every stimulation cycle, image size randomly varied between 80% and 120% in order to even further minimize pixel overlap (e.g., eyes falling in the same location) between consecutive stimuli (Dzhelyova & Rossion, 2014; Liu-Shuang et al., 2014). Face stimuli were presented either at upright or inverted orientation in each sequence, six times each. The order of the face orientation conditions was randomized across participants. Participants had to do an orthogonal task by responding to the color change of a central fixation cross (from black to red, nonperiodic, appearing during 200 msec). The whole recording took about 20 min (about seven minutes per orientation for visual stimulation, and breaks).

2.3.2. *EEG acquisition*

The experiment was run in a quiet, and low-lit room. The stimulation sequences were presented on an LED monitor (BenQ XL2420T) with a 1600 × 900 window resolution and a 120 Hz refresh rate. Stimuli were presented centrally on the screen. High-density 128-channel EEG was acquired with the ActiveTwo Biosemi system (Biosemi, Amsterdam, The Netherlands) at a 512 Hz sampling rate. The magnitude of the offset of all electrodes, referenced to the common mode sense (CMS), was held below 30 μV. Vertical and horizontal electro-oculogram (EOG) was recorded using four additional flat-type active-electrodes: two electrodes above and below the participant's right orbit and two lateral to the external canthi of the two eyes.

2.4. *Analysis*

2.4.1. *Preprocessing*

EEG data was analyzed as in previous studies using this approach (e.g., Liu-Shuang et al., 2014; Retter & Rossion, 2016; Zimmermann et al., 2019), with the open source software Letswave 5 (https://github.com/NOCIONS/Letswave5), running in MATLAB R2013a (MathWorks, USA). EEG data was first band-pass filtered between .05 and 100 Hz with a 4th order zero-phase Butterworth filter and then down-sampled to 256 Hz for the ease of processing. The data sequence was then segmented relative to the starting trigger of each trial, with an additional 2 sec before and after each sequence (−2–76 sec). Eyeblink artifacts more than .2 times/s on average (Retter & Rossion, 2016) were corrected by applying independent component analysis (ICA) on 8 participants (across two experiments). Individual channels with artifacts were interpolated by their three neighboring channels. The maximum interpolated channels for each participant was 6 (2.5 ± 1.9 on average). The cleaned-up data was then referenced to the average of all 128 electrodes.

2.4.2. *Frequency domain analysis*

The preprocessed data were cropped again into epochs with an integer number of cycles of familiar face presentation cycles (Retter & Rossion, 2016). The first and last 2 sec of each presentation sequence were discarded to remove eye-movements and muscle artifacts related to abrupt onset and offset of the flickering stimuli. The resulting cropped epochs were 68.84 sec long and contained exactly 59 face presentation cycles. A Fast Fourier Transform (FFT) was applied and the amplitude spectra were extracted, with a frequency resolution of .0145 Hz (1/68.84 sec).

Baseline EEG activity was estimated as in previous studies (e.g., Liu-Shuang, Torfs, & Rossion, 2016, 2014; Retter & Rossion, 2016; Zimmermann et al., 2019), with the neighbouring 20 bins surrounding the frequency bins of interest (10 bins by each side, excluding the immediately adjacent bins in case of remaining spectral leakage, and the local maximum and minimum amplitude bins to avoid projecting the signal in the noise EEG spectrum). Then, two methods were applied for baseline correction of the EEG responses: (1) division by the EEG noise to show EEG spectrum in signal-to-noise ratio (SNR), allowing to better visualize small responses and (2) Subtraction of the EEG noise (baseline subtraction, SBL) to quantify responses in μV across summed harmonics (Retter & Rossion, 2016; Rossion, Retter, & Liu-Shuang, 2020).

For the two presentation frequencies (6 Hz and .86 Hz), there were responses reflected at multiple harmonics, in line with previous studies (e.g., Liu-Shuang et al., 2014; Retter & Rossion, 2016; Zimmermann et al., 2019). Harmonics were selected according to the grand-averaged response patterns across all participants, all channels and both face orientation conditions (Retter & Rossion, 2016; Zimmermann et al., 2019). We computed a z-score at each discrete frequency bin, with a threshold at 2.3 ($p < .01$, one-tailed, signal > noise) to select significant harmonics (Retter & Rossion, 2016; Zimmermann et al., 2019). In this way, the first 6 significant harmonics (i.e., .86 Hz, 1.71 Hz, 2.57 Hz, 3.43 Hz, 4.29 Hz, and 5.14 Hz) were identified, and summed to quantify the FFR response. The general visual responses at 6 Hz were identified with the same approach and quantified by summing the first 8 significant harmonics (i.e., 6 Hz, 12 Hz, and up to 48 Hz).

We statistically tested neural responses at the group level over across the whole scalp channels and at local regions-of-interest (ROIs) where the two responses at .86 Hz and 6 Hz (and their harmonics) reached to maxima, consistent with previous studies with the same frequency-tagging paradigm measuring familiar face identity recognition (Yan et al., 2020; Zimmermann et al., 2019), and unfamiliar face individuation (Rossion et al., 2020 for review). Therefore, a middle occipital ROI was defined with 9 middle posterior channels (Oz, OIz, Iz, O1&2, POI1&2, I1&2), and a bilateral occipito-temporal (OT) ROI with 10 posterior channels P7&8, P9&10, PO7&8, PO9&10, PO11&12. We also split the OT ROI into left OT ROI (P7, P9, PO7, PO9, PO11) and right OT ROI (P8, P10, PO8, PO10, PO12) to investigate the hemispheric differences in the FFR response. In addition, given that there were scalp topography differences across individuals (Yan et al., 2020; Zimmermann et al.,

2019), the FFR response was also quantified individually with the 10 channels showing the largest responses for each individual participant, independently for each face orientation condition. The distribution of these 10 channels across participants is shown in Figure S1. For the upright face condition, a majority of the selected channels were located over bilateral OT ROIs (about 70%) across participants, while for the inverted face condition, the channels showing the largest responses were widespread with only about 18% of the channels located over bilateral OT regions.

To measure whether each individual's FFR response over different ROIs at .86 Hz (and harmonics) was significantly higher than EEG noise, we calculated the z-score based on the summed-harmonic response at .86 Hz and its 20 neighbouring bins. A significant recognition response was identified at a z-score threshold of 1.64 ($p < .05$, one-tailed, signal > noise).

2.4.3. *Response correlation*

We compared the response patterns to the two face conditions across individual participants of both the FFR response and the general visual response. Correlation analyses were calculated with summed-harmonic response amplitude (μV).

2.4.4. *Time domain analysis*

The spatio-temporal dynamics of the FFR response was investigated with similar methods as previous studies using the same frequency-tagging approach (Jacques, Retter, & Rossion, 2016; Retter & Rossion, 2016; Yan et al., 2019; see Rossion et al., 2020 for review). Referenced EEG signal were low-pass filtered with a 30 Hz cut-off (4th order Butterworth filter), and then cropped into an integer number of cycles of the familiar face presentation frequency (from 2 to 70.84 sec, 59 face presentation cycles). After that, the general face

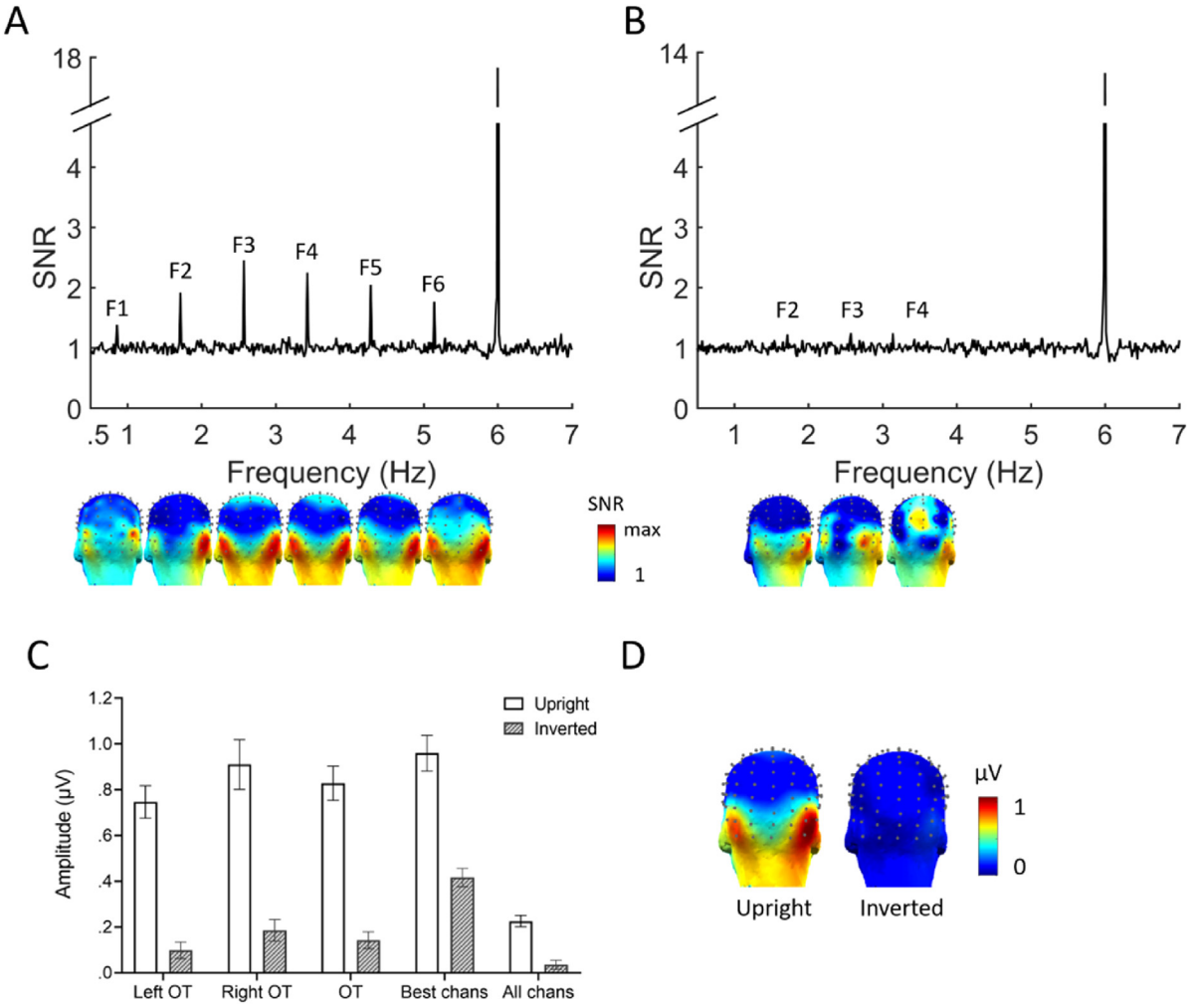

Fig. 2 – Grand-averaged EEG spectra of the FFR response, in SNR, over OT ROI, for upright (A) and inverted (B) faces. Three-D scalp topography maps (posterior view) are shown below each significant harmonic. The color scale shows the response range from 1 to the maximum SNR of each harmonic. A SNR peak of 2 corresponds to 100% increase of signal. C. Grand-averaged baseline-corrected amplitudes for both face orientation conditions, over left and right OT ROI, best 10 channels defined separately for each orientation condition, and across all scalp channels. Error bars indicate standard errors of the mean. D. Three-D scalp topography maps for summed-harmonic FFR responses for both conditions.

presentation frequency and its first 5 harmonics (up to 30 Hz) was removed with narrow band notch-filtering (width = .05). The EEG waveforms were then segmented into smaller epochs containing 7 stimulation cycles (i.e., 1167 msec), which containing 6 unfamiliar face presentations (U) and one familiar face presentation (F) with a pattern of 'UFUUUUU'. Epochs were averaged and baseline-corrected relative to the first unfamiliar face stimulus presentation (-167 – 0 msec). This analysis was conducted on individual participant before averaging to the group level.

Since the stimuli were progressively revealed through sinusoidal contrast modulation (Fig. 1; Figure S3A), we estimated the true stimulus onset (i.e., the level of stimulus contrast sufficient to trigger a FFR response) by comparing the sinewave stimulation with a squarewave (50% duty cycle, see Retter, Jiang, Webster, & Rossion, 2018) stimulation in an independent individual recording (20 sequences with upright stimuli only). The delay between the two stimulation modes was of about 41.7 msec (Figure S3B), corresponding to 50% of contrast. A correction (i.e., subtraction) of 41.7 msec to all individual data was therefore applied to estimate the true stimulus onset time (Fig. 6).

To determine the time-windows that showed significant response difference to the periodic presentation of familiar faces between the upright and inverted face conditions, we ran a cluster-based nonparametirc permutation *t*-test on the post-stimulus onset time-points (0 - 1000 msec after stimulus onset) with the Fieldtrip toolbox (5000 permutations with the Monte Carlo method, minimum 3 neighborhood channels). The permutation *t*-test was run with a threshold of $p < .05$ (two-tailed) for both the cluster statistic and the permutation test, using the percentile cut-off of the maximum of summed t-statistics within clusters (Maris & Oostenveld, 2007; Yan et al., 2019). Only participants who showed significant face inversion effect over the OT ROI were included in the permutation analysis.

2.4.5. *Behavioral analysis*

For the fixation color detection task, response times (RTs) were calculated relative to the onset of color change.

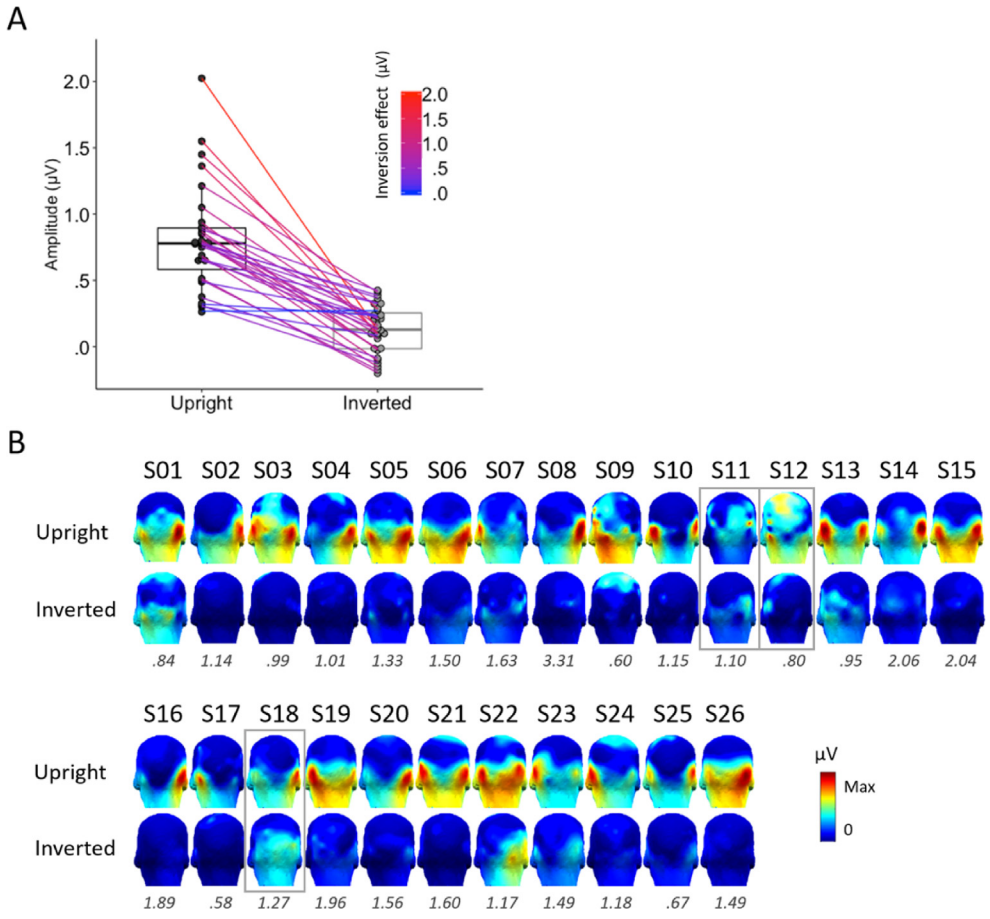

Fig. 3 – A. Box plot with individual points showing individual FFR responses over the OT ROI for both face conditions (Upright with black points and Inverted with gray points). Each individual participant's responses of two conditions are combined by a line with its color scaled by the size of the face inversion effect. B. Three-D scalp topographies showing FFR responses of both face conditions. The maximum response amplitude (μV) of each individual participant across two conditions is shown underneath the corresponding scalp maps. The three participants with no significant face inversion effect are indicated with gray boxes, showing that their response is nevertheless larger for upright than inverted faces (see Table S1 & S2).

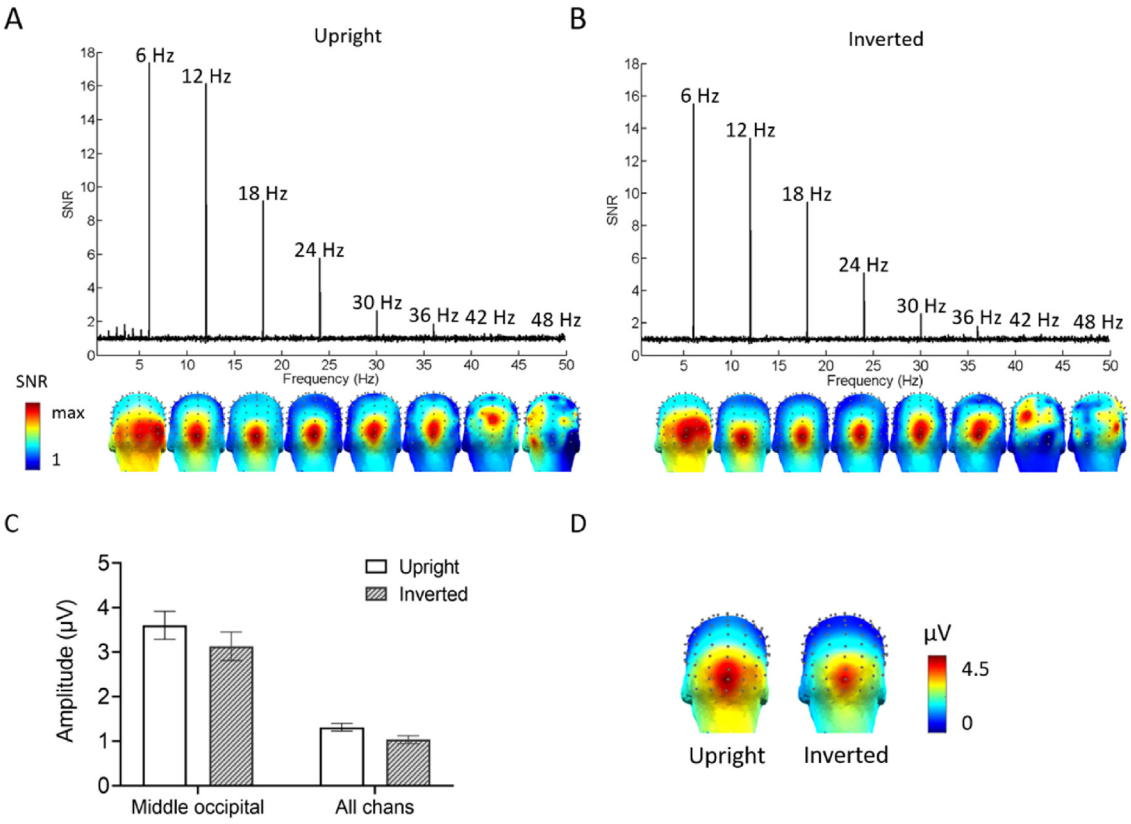

Fig. 4 – Grand-averaged general face presentation response in SNR for both the upright (A) and inverted (B) face condition. Three-D scalp topography maps are shown below each significant harmonic. The color scale shows the response range from 1 to the maximum SNR of each harmonic. C. Grand-averaged baseline-corrected amplitudes for both face orientation conditions, over middle occipital ROI, and across all scalp channels. Error bars indicate standard errors of the mean. D. Three-D scalp topography maps for summed-harmonic general face presentation responses of both conditions.

Responses were considered correct if they occurred between 150 msec and 1000 msec following target onset.

3. Results

Since separate analyses of each version of the experiment showed similar response patterns, and there was no FFR response difference between two experimental versions ($p > .1$) (see the supplemental data file for separate analysis of each version and their comparison), we report the results collapsed across the two versions, for a total of 26 participants. Note that a power analysis was run for each version of the experiment with G*Power (Faul, Erdfelder, Lang, & Buchner, 2007). The main effect of face orientation in each version is closing to 1 (see supplemental data file), indicating that with the current paradigm and sample size, we are able to measure a reliable FFR response.

3.1. Behavioral results

Participants performed equally well across two face orientation conditions, both on accuracy rates and correct response times (RTs). Separate *t*-test on the two measures showed no difference between the two face orientation conditions: Accuracy rates: $t_{(25)} = .65$, $p > .1$ (Upright: 98.3 ± 2.2%; Inverted: 98.6 ± 3.1%); RTs: $t_{(25)} = .84$, $p > .1$ (Upright: 476 ± 48 msec; Inverted: 466 ± 48 msec).

3.2. EEG results

3.2.1. Robust FFR response at .86 Hz and harmonics

A clear FFR response was found at the group level, especially over the bilateral low occipito-temporal regions: the SNR was very high for upright faces at .86 Hz and 5 harmonics (e.g., 1.71 Hz, 2.57 Hz, etc.) (Fig. 2A). Responses over the same regions were negligible when the exact same conditions of stimulation were presented at the inverted orientation, with only three weakly significant harmonics (Fig. 2B). While the FFR response for inverted faces over the OT ROI was significantly above 0, $t_{(25)} = 3.86$, $p = .001$, it was only of about 17% of the response to upright faces (Upright: $M = .83 \pm .41$ μV; Inverted: $M = .14 \pm .19$ μV). A two-way repeated ANOVA on the mean amplitude over OT region with *Orientation* (Upright, Inverted) and *Hemisphere* (Left, Right) as within-subjects factors showed a large main effect of *Orientation*, $F(1,25) = 71.57$,

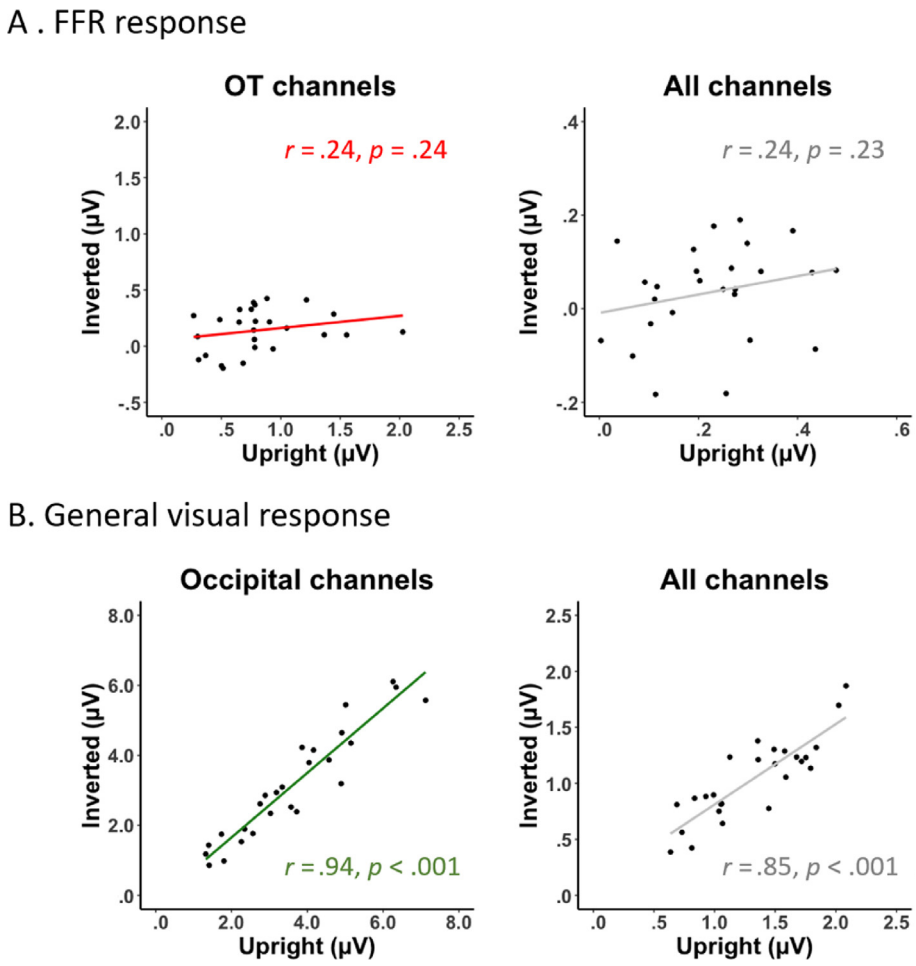

Fig. 5 – Scatterplots showing correlation of the response amplitudes (μV) to upright and inverted faces over different ROIs for the FFR response (A) and the general visual response (B).

$p < .001$, $\eta^2 = .74$, a borderline significant main effect of *Hemisphere* (F (1,25) = 4, $p = .06$, $\eta^2 = .14$), due to a right hemisphere advantage (Left: $M = .42 \pm .23$ μV; Right: $M = .55 \pm .35$ μV). The interaction of *Orientation* × *Hemisphere* was not significant, F (1,25) = .53, $p = .48$, $\eta^2 = .02$ (Fig. 2C).

The FFR responses was also compared across all 128 channels between the two orientation conditions, showing again a much larger response for upright images, $t_{(25)} = 6.86$, $p < .001$ (Upright: $M = .23 \pm .13$ μV; Inverted: $M = .04 \pm .10$ μV; about 17% of the response to upright faces). The same response pattern replicated over the 10 channels with the largest responses defined separately for each condition, $t_{(25)} = 7.27$, $p < .001$ (Upright: $M = .96 \pm .4$ μV; Inverted: $M = .42 \pm .2$ μV; about 44% of the response to upright faces).

3.2.2. *Robust neural index of FFR in each individual*

While the scalp topographies were quite similar, the amplitude of the FFR response varied substantially across individuals (Fig. 3). Impressively, when considering the response over the same bilateral OT regions for all participants, we found a significant FFR response for upright faces in all of the 26 participants at a threshold of $z > 1.64$ ($p < .05$, one tailed). Even at a more conservative threshold ($z > 2.33$, $p < .01$, one tailed), all 26 participants showed a significant FFR response. All participants also showed a larger response to upright than inverted faces, and this response was significantly larger ($z > 1.64$, $p < .05$) for 23 of the 26 participants for upright as compared to inverted faces (Fig. 3). The response amplitudes and z-scores for each individual participant for each condition over different ROIs are shown in Table S1 & S2.

3.2.3. *Index of general face presentation response at 6 Hz*

Significant responses at 6 Hz and the following 7 harmonics (i.e., up to 48 Hz) were consistently found across the two face orientation conditions (Fig. 4). For both orientations, responses at 6 Hz were found over the occipito-temporal regions but mainly on middle occipital regions (Zimmermann et al., 2019). Responses at the second harmonic and subsequent harmonics focused on the medial occipital cortex. Over the middle occipital ROI, the response to inverted faces reached 87% of the response to upright faces, $t_{(25)} = 4.48$, $p < .01$ (Upright: 3.6 ± 1.6 μV; Inverted: 3.13 ± 1.57 μV). Across all 128

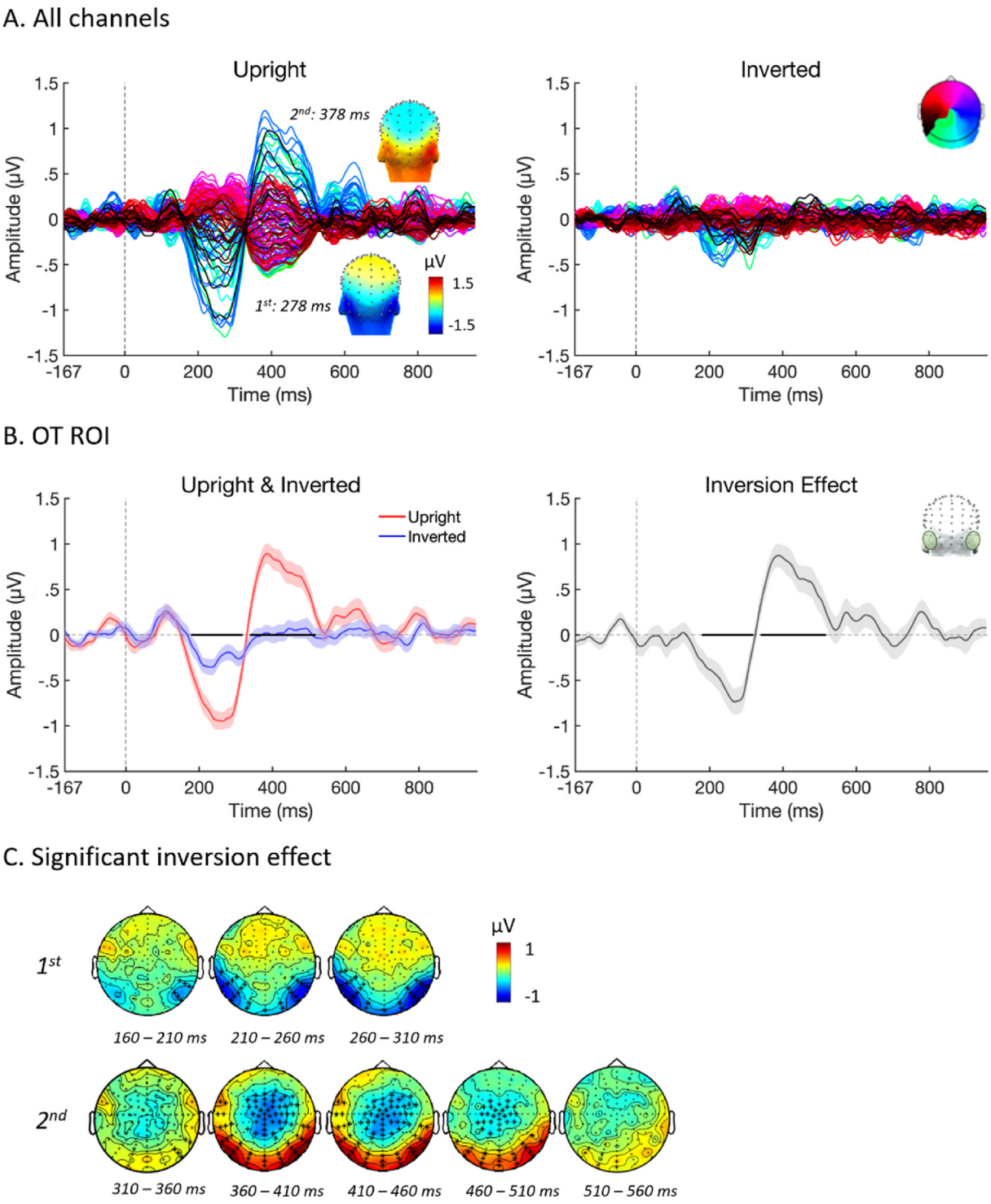

Fig. 6 – Time course of the grand-averaged FFR response. A. FFR responses of both face orientation conditions (left panel: Upright, right panel: Inverted) across all 128 channels. For the upright face condition, there are two deflections (shown also with scalp topographies) from about 160 msec continuing up to until 560 msec after stimulus onset. The two-dimensional head map (viewed from the top of the head) over the upper right corner represents the color codes of the channels. B. Averaged waveform over bilateral OT ROI for two face conditions (left panel) and their difference wave (right panel). Shaded areas represent ±1 standard error of the mean across participants. Time windows showing significant face inversion effect are indicated with thick black lines along the x-axis. The early negative component was shown from about 180 to 320 msec, and a later positivity from approximately 340-520 msec. C. Two-D scalp topographies showing significant face inversion effect within 50 msec time windows. Significant electrode clusters are indicated with black asterisks.

channels, the general visual response to inverted faces was of about 79% of the response to upright faces, with this difference being significant, $t_{(25)} = 6.37$, $p < .001$ (Upright: 1.31 ± .43 μV; Inverted: 1.04 ± .36 μV). In addition, we tested the response at the first harmonic over different ROIs. Over bilateral OT ROIs, a repeated-ANOVA with *Hemisphere* (Left, Right) and *Orientation* (Upright, Inverted) as within-subjects factors showed a significant main effect of Hemisphere, suggesting that the response in the left OT regions reached about 72% of the response to the right OT regions, F (1,25) = 9.73, $p < .01$, $\eta^2 = .28$ (Left: 1.39 ± .86 μV; Right: 1.92 ± .82 μV). There was also a main effect of *Orientation*, with the response to the inverted faces of about 74% of the response to the upright faces, F (1,25) = 17.3, $p < .001$, $\eta^2 = .41$ (Upright: 1.90 ± .96 μV; Inverted: 1.41 ± .56 μV). The interaction between *Hemisphere* × *Condition* was not significant ($p > .1$). Analysis of the response over the middle occipital ROI showed a significant larger response to the upright faces versus inverted faces, $t_{(25)} = 2.05$, $p = .05$. (Upright: 1.65 ± .92 μV; Inverted: 1.45 ± .83 μV). For the remaining harmonics (i.e., 12, 18, up to 48 Hz), there was also a response difference between upright an inverted face condition over the occipital ROI, $t_{(25)} = 5.97$, $p < .001$. (Upright: 1.96 ± 1.04 μV; Inverted: 1.68 ± 1.04 μV).

3.2.4. *Response correlation of upright and inverted faces*

Using variability of the FFR response across individuals, we explored the response relationship between two face orientation conditions for both the FFR response (Fig. 5A) and the general visual response (Fig. 5B). No significant correlations between upright and inverted faces were found for the FFR response, as measured across all channels or the OT ROIs with *ps* > .23 (*rs* = .24). When extreme values over the OT channels or all channels were removed, there were still no significant correlations (both *ps* > .1). This means that the amplitude of the FFR response to upright faces is unrelated to the amplitude of the response to inverted faces. However, for the general visual responses over the middle occipital and across all 128 channels, there were highly significant correlations between responses to upright and inverted faces (both *ps* < .001).

3.2.5. *Spatio-temporal dynamics of the FFR response*

The time domain analysis showed two major response deflections for the upright familiar faces, with no clear response deflections shown for inverted faces (Fig. 6A). These wide deflections were maximal over bilateral occipito-temporal regions, consistent with the results of the frequency domain analysis. A negative deflection was found starting at around 160 msec after stimulus onset, peaking at approximately 278 msec. A second positive component was observed at about 335 msec after stimulus onset, peaking at approximately 378 msec, with a prolonged deflection until about 560 msec. Fig. 6B shows the averaged waveform over the bilateral OT ROI at two face conditions (left panel) and their difference wave (right panel). Significant face inversion effect (with the Monte Carlo method, see Methods part) were detected at two time windows: an early negativity at 180–320 msec and a later positivity at 340–520 msec, respectively (Fig. 6C). During the 340–480 msec time window, a significant inverse polarity response was also observed, but with the negative amplitude distributed over many channels of the central parietal region.

4. Discussion

We report a neural FFR response across different identities, extending recent observations with the same approach in which the same (famous) facial identity, across variable image changes, was repeated periodically among a rapid train of variable unfamiliar faces (Zimmermann et al., 2019; Campbell et al., 2020; Yan et al., 2020). The present FFR response is obtained without an explicit face recognition task in only seven minutes for an individual participant and, remarkably, is significant in each of the 26 participants tested in the study, even at a conservative statistical threshold ($p < .01$). While the present experiment required considerable time to set-up the high-density EEG coverage (i.e., 128 channels) on the participant's head before data recording, the bulk of the FFR response focuses on a relatively small subset of channels over the bilateral occipito-temporal regions, with a high degree of homogeneity across individual brains (Fig. 3). In fact, a selection of the channels associated with the largest response independently for every individual participant does not lead to a significantly larger response than the response obtained on the right hemispheric OT region defined the same way for all participants (Fig. 2C). Hence, a few channels located over this region appears to be sufficient to record the maximal FFR response in a single individual (as for unfamiliar face individuation responses in FPVS, see Rossion et al., 2020). Compared to previous studies that have contrasted neural responses to familiar and unfamiliar faces as reviewed in the introduction, the robustness of the reported data is unprecedented, yet is in line with the large behavioral differences that have been described between natural images of unfamiliar and familiar (especially highly well-known celebrities) faces (Jenkins et al., 2011; Ritchie, Smith, et al., 2015).

Why is the neural FFR so robust in the present paradigm? First, we describe a *compact* response in the EEG frequency-domain (the main goal of the study), which encompasses any type of reliable electrophysiological difference between familiar and unfamiliar faces (i.e., increases, decreases, change in phase; see Rossion et al., 2020). Second, the FFR response is based on 6 (stimulation sequences) × 59 famous face onsets, so that it represents the average of a very large number (i.e., 354) of recorded trials over only about 7 min of stimulation (with each specific image being presented on average 3 times). Note that a ratio of 1/7 was used here to obtain a cleaner baseline in the time-domain (i.e., 1.17 sec between famous faces), but the results indicate that a 1/5 ratio at 6 Hz (i.e., .833 sec between famous faces) would be sufficient to capture all of the FFR response, allowing even more trials to be collected during a stimulation sequence and an even higher SNR. Last but not least, unlike standard ERP studies or frequency-tagging studies comparing familiar and unfamiliar faces indirectly (e.g., Collins, Robinson, & Behrmann, 2018; Lui, Lui, Wong, & Rosenfeld, 2018), the FFR response at .86 Hz and specific harmonics recorded here originates from a *direct contrast* between familiar and unfamiliar faces. That is,

common processes to the two kinds of stimuli project to the 6 Hz response and its harmonics, and no post-hoc subtraction is required to obtain the FFR response. While the present approach does not provide separate EEG waveforms for familiar and unfamiliar faces and thus may not allow extracting "representational codes" separately for familiar and unfamiliar faces, it is based on the view that the nervous system's primary function in its interaction with the environment is not in coding different stimuli in isolation, but in producing *discriminative* (i.e., selective) responses that can be reproduced (i.e., *generalized*) adaptively. An objective and sensitive measure of a neural response reflecting directly this categorization/recognition function should therefore be a primary goal of cognitive neuroscience research, insofar as it can lead to better characterization and understanding of this function.

Is the large difference between familiar and unfamiliar faces due to the recruitment of distinct visual representations for the two kinds of faces (Andrews, Jenkins, Cursiter, & Burton, 2015; Burton, Jenkins, & Schweinberger, 2011; Longmore, Liu, & Young, 2008; Ramon, 2015a, 2015b; Ramon & Van Belle, 2016; Young & Burton, 2018) or to familiar faces only being associated with semantic, affective and verbal information (Dixon, Bub, & Arguin, 1997; Rossion, 2018; Schwartz & Yovel, 2016)? Even if the FFR response is located over the occipito-temporal cortex with a (slight) right hemispheric advantage, and emerges relatively early (i.e., 160–200 msec as a conservative estimation, see below), the present study cannot unequivocally answer this question: the differential response could well be due to the periodic activity for famous faces of multimodal populations of neurons in the anterior section of the ventral occipito-temporal cortex that have been shaped by our knowledge of the environment (i.e., semantic memory) (Lambon Ralph, 2012; Rice, Hoffman, & Ralph, 2015). However, by producing a relatively straightforward and highly sensitive implicit FFR measure, our paradigm offers a unique opportunity to contrast these views in future studies. For instance, one could familiarize people with natural images of a set of facial identities with or without semantic/affective/verbal cues associated (e.g., Schwartz & Yovel, 2016), or with overlapping or distinct semantic information (Dixon et al., 1997), and then test the FFR response with a new set of images of these identities inserted in a train of unfamiliar faces.

While the familiar face identity response reported previously (Zimmermann et al., 2019; Campbell et al., 2020; Yan et al., 2020) could be partly attributed to shared physical characteristics between the periodically repeated images of a given famous identity (e.g., J. Dujardin's facial images), this is virtually impossible here since the response is due to faces of six famous identities that are quite different physically. Supporting this, most of the FFR response (i.e., 83% over occipito-temporal channels) is eliminated when the images are presented upside-down, even though physical differences between familiar and unfamiliar faces remain strictly identical following picture-plane inversion. Importantly, this does not imply that 17% of the FFR response is due to low-level visual characteristics: even when they are presented at upside-down orientation, faces can be recognized as being familiar above chance level (Besson et al., 2017; Busigny & Rossion, 2010; Collishaw & Hole, 2000). However, the effect indicates unambiguously that 83% of the FFR response is not due to different physical characteristics of the familiar and unfamiliar faces independently of an observer's knowledge, i.e. his/her memory of the familiar identities experienced at upright orientation. Moreover, the lack of significant correlation between the FFR response for upright and inverted faces across participants – despite a very high correlation for generic visual responses – (Fig. 5) supports the view that the participants who can recognize familiar faces upside-down and contribute more to the FFR response at this unusual orientation do not necessarily generate a larger response when faces are presented at the experienced upright orientation. This is in contrast with the significant correlation ($r = .55$, $p < .001$) observed across individuals' amplitudes for a face individuation response measured on upright and inverted *unfamiliar* faces with the same frequency-tagging approach (Rossion et al., 2020), replicating behavioral observations (Megreya & Burton, 2006). Importantly, the contrast between a significant correlation for unfamiliar faces and a non-significant correlation for familiar faces does not imply that unfamiliar faces are processed like inverted faces (i.e., the non-shared variance remains substantial). Rather, it can be attributed to the fact that unfamiliar face individuation *has* to be based on processes/representations of visual inputs only, which can be partly shared for the two orientations, while selective responses to familiar faces also depend heavily on interindividual variability in terms of semantic knowledge of the identities.

In the present study, we also describe the FFR response in the time-domain, with inverted faces used to fully isolate the high-level aspect of this response (Fig. 6). This time-domain response is expressed over occipito-temporal electrodes in the form of two deflections, a negative polarity between about 160 msec and 320 msec followed by a positive deflection between 340 and 560 msec. This pattern resembles the two main deflections observed when individuating pictures of unfamiliar faces (Rossion et al., 2020), although the neural populations subtending these deflections could be different. This timing is compatible with studies that have reported face familiarity effects as early as the face-selective N170 as reviewed in the introduction (e.g., Barragan-Jason et al., 2015; Caharel et al., 2005; Jemel et al., 2010; Wild-Wall et al., 2008), yet such early effects are generally weak, inconsistent across studies, and mainly found for pictures of personally familiar faces. It is also in line with explicit go/nogo familiarity responses emerging no later than 200 msec (Barragan-Jason et al., 2015; Caharel, Ramon, & Rossion, 2014) and, more generally, with the enhanced N250 found for familiar as compared to unfamiliar faces over the occipito-temporal region (e.g., Barragan-Jason et al., 2015; Gosling & Eimer, 2011; Jemel et al., 2010; Wiese et al., 2019). Interestingly, rather than reporting separate effects on different ERP components (i.e., N170 followed by N250), our data obtained during fast periodic visual stimulation, which reflect only differential (i.e., contrast) EEG responses, suggest a single occipito-temporal face familiarity negative deflection, lasting from about 160 msec to about 320 msec following stimulus onset.

Overall, the present FFR response extends beyond 320 msec, lasting until about 560 msec post-stimulus onset. This is in line with the spread of these effects across various

components in standard ERP studies as reviewed in the introduction, suggesting that the FFR response involves deep prolonged activation of semantic, verbal and affective information linked to familiar face representations. However, unlike late FFR effects that appear to be indefinitely prolonged in standard ERP studies (e.g., beyond 700 msec in Gosling & Eimer, 2011; Wiese et al., 2019), presenting each famous face inserted in a rapid train of other (here, unfamiliar) faces in the present paradigm leads to a clear return to baseline and a precise temporal definition of the FFR response duration (Fig. 6).

In summary, we propose a sensitive, objective, and straightforward approach to implicitly measure a key cognitive brain function: familiar face recognition. A significant FFR neural response can be measured in the EEG frequency domain over bilateral occipito-temporal region with a (slight) right hemisphere advantage, being significant in each individual participant. With an implicit task, our study offers robust neural evidence of the large behavioral differences between famous and nonfamous faces that are extensively described in behavioral research. It also opens new perspectives for investigating the functional neural networks of FFR by combining this frequency-tagging approach with fMRI (e.g., Gao, Gentile, & Rossion, 2018) and intracerebral human recordings (e.g., Jonas et al., 2016). Besides, this approach could be extended in future studies to investigate biological markers for personally familiar face recognition, the effect of face learning, and multi-modality person recognition (e.g., names, voices, and the interactions of the modalities) (e.g., Volfart, Jonas, Maillard, Colnat-Coulbois, & Rossion, 2020). It could also be applied in forensic and clinical settings to assess one's ability to recognize human faces, including super-recognizers, and people with developmental difficulties at face recognition.

Credit author statement

X.Y. designed the experiment, collected data, analyzed the data, intepreted the data, and wrote the manuscript.

B.R. designed the experiment, contributed to the data analysis, intepreted the data, and wrote the manuscript.

Data and code availability

The EEG data were analyzed using the open source Letswave software package (https://github.com/NOCIONS/Letswave5), running in MATLAB R2013a (MathWorks, USA). Data analysis steps are available at: https://osf.io/527gf/.

The preprocessed time-domain data and behavioural data are available at: https://osf.io/527gf/.

Stimuli: all face stimuli we used in the experiment were searched and downloaded online through Google Image. The name of the face identities used in the first version of the experiment is provided in the method part. Legal copyright restrictions prevent us from making the face stimuli publicly available or sharing them on request with any individual outside the author team.

The experimental design was implemented using custom software written in Java. The code is available at: https://osf.io/527gf/

No part of the study procedures was pre-registered prior to the research being conducted.

We report how we determined our sample size, all data exclusions (if any), all inclusion/exclusion criteria, whether inclusion/exclusion criteria were established prior to data analysis, all manipulations, and all measures in the study.

Declaration of Competing Interest

The authors declare no competing interests.

Acknowledgement

This study was supported by a co-funded initiative by the Université Catholique de Louvain and the Marie Curie Actions of the European Commission award (grant no. F211800013) and a postdoctoral fellowship from the Region Grand Est to X. Y.

Supplementary data

Supplementary data to this article can be found online at https://doi.org/10.1016/j.cortex.2020.08.016.

Open practices

The study in this article earned an Open Data badge for transparent practices. Materials and data for the study are available at https://github.com/NOCIONS/letswave6/wiki.

REFERENCES

Andrews, S., Jenkins, R., Cursiter, H., & Burton, A. M. (2015). Telling faces together: Learning new faces through exposure to multiple instances. *Quarterly Journal of Experimental Psychology, 68*(10), 2041–2050.

Axelrod, V., & Yovel, G. (2013). The challenge of localizing the anterior temporal face area: A possible solution. *Neuroimage, 81*, 371–380.

Barragan-Jason, G., Cauchoix, M., & Barbeau, E. J. (2015). The neural speed of familiar face recognition. *Neuropsychologia, 75*, 390–401.

Begleiter, H., Porjesz, B., & Wang, W. (1995). Event-related brain potentials differentiate priming and recognition to familiar and unfamiliar faces. *Electroencephalography and Clinical Neurophysiology, 94*(1), 41–49.

Bentin, S., Allison, T., Puce, A., Perez, E., & McCarthy, G. (1996). Electrophysiological studies of face perception in humans. *Journal of Cognitive Neuroscience, 8*, 551–565.

Bentin, S., & Deouell, L. Y. (2000). Structural encoding and identification in face processing: ERP evidence for separate mechanisms. *Cognitive Neuropsychology, 17*(1–3), 35–55.

Besson, G., Barragan-Jason, G., Thorpe, S. J., Fabre-Thorpe, M., Puma, S., Ceccaldi, M., & Barbeau, E. J. (2017). From face processing to face recognition: Comparing three different processing levels. *Cognition, 158*, 33–43.

Bruce, V. (1982). Changing faces: Visual and non-visual coding processes in face recognition. *British Journal of Psychology, 73*(1), 105–116.

Bruce, V., Henderson, Z., Newman, C., & Burton, A. M. (2001). Matching identities of familiar and unfamiliar faces caught on CCTV images. *Journal of Experimental Psychology: Applied, 7*(3), 207–218.

Burton, A. M., Bruce, V., & Hancock, P. J. (1999). From pixels to people: A model of familiar face recognition. *Cognitive Science, 23*(1), 1–31.

Burton, A. M., Jenkins, R., & Schweinberger, S. R. (2011). Mental representations of familiar faces. *British Journal of Psychology, 102*(4), 943–958.

Burton, A. M., Kramer, R. S., Ritchie, K. L., & Jenkins, R. (2016). Identity from variation: Representations of faces derived from multiple instances. *Cognitive Science, 40*(1), 202–223.

Busigny, T., & Rossion, B. (2010). Acquired prosopagnosia abolishes the face inversion effect. *Cortex, 46*(8), 965–981.

Caharel, S., Bernard, C., Thibaut, F., Haouzir, S., Di Maggio-Clozel, C., Allio, G., & Rebaï, M. (2007). The effects of familiarity and emotional expression on face processing examined by ERPs in patients with schizophrenia. *Schizophrenia Research, 95*(1–3), 186–196.

Caharel, S., Courtay, N., Bernard, C., Lalonde, R., & Rebaï, M. (2005). Familiarity and emotional expression influence an early stage of face processing: An electrophysiological study. *Brain and Cognition, 59*(1), 96–100.

Caharel, S., Poiroux, S., Bernard, C., Thibaut, F., Lalonde, R., & Rebai, M. (2002). ERPs associated with familiarity and degree of familiarity during face recognition. *International Journal of Neuroscience, 112*(12), 1499–1512.

Caharel, S., Ramon, M., & Rossion, B. (2014). Face familiarity decisions take 200 msec in the human brain: Electrophysiological evidence from a go/no-go speeded task. *Journal of Cognitive Neuroscience, 26*(1), 81–95.

Campbell, A., Louw, R., Michniak, E., & Tanaka, J. W. (2020). Identity-specific neural responses to three categories of face familiarity (own, friend, stranger) using fast periodic visual stimulation. *Neuropsychologia, 141*, 107415.

Collins, E., Robinson, A. K., & Behrmann, M. (2018). Distinct neural processes for the perception of familiar versus unfamiliar faces along the visual hierarchy revealed by EEG. *NeuroImage, 181*, 120–131.

Collishaw, S. M., & Hole, G. J. (2000). Featural and configurational processes in the recognition of faces of different familiarity. *Perception, 29*(8), 893–909.

Dixon, M., Bub, D. N., & Arguin, M. (1997). The interaction of object form and object M eaning in the identification performance of a patient with category-specific visual agnosia. *Cognitive Neuropsychology, 14*(8), 1085–1130.

Dzhelyova, M., & Rossion, B. (2014). The effect of parametric stimulus size variation on individual face discrimination indexed by fast periodic visual stimulation. *BMC Neuroscience, 15*(1), 87.

Eimer, M. (2000). Event-related brain potentials distinguish processing stages involved in face perception and recognition. *Clinical Neurophysiology, 111*, 694–705.

Ewbank, M. P., & Andrews, T. J. (2008). Differential sensitivity for viewpoint between familiar and unfamiliar faces in human visual cortex. *Neuroimage, 40*(4), 1857–1870.

Faul, F., Erdfelder, E., Lang, A. G., & Buchner, A. (2007). G* power 3: A flexible statistical power analysis program for the social, behavioral, and biomedical sciences. *Behavior Research Methods, 39*(2), 175–191.

Gao, X., Gentile, F., & Rossion, B. (2018). Fast periodic stimulation (FPS): A highly effective approach in fMRI brain mapping. *Brain Structure and Function, 223*(5), 2433–2454.

Gobbini, M. I., & Haxby, J. V. (2007). Neural systems for recognition of familiar faces. *Neuropsychologia, 45*(1), 32–41.

Gobbini, M. I., Leibenluft, E., Santiago, N., & Haxby, J. V. (2004). Social and emotional attachment in the neural representation of faces. *Neuroimage, 22*(4), 1628–1635.

Gorno-Tempini, M. L., & Price, C. J. (2001). Identification of famous faces and buildings: A functional neuroimaging study of semantically unique items. *Brain, 124*(10), 2087–2097.

Gosling, A., & Eimer, M. (2011). An event-related brain potential study of explicit face recognition. *Neuropsychologia, 49*(9), 2736–2745.

Hancock, P. J., Bruce, V., & Burton, A. M. (2000). Recognition of unfamiliar faces. *Trends in Cognitive Sciences, 4*(9), 330–337.

Henson, R. N. A., Shallice, T., Gorno-Tempini, M. L., & Dolan, R. J. (2002). Face repetition effects in implicit and explicit memory tests as measured by fMRI. *Cerebral Cortex, 12*(2), 178–186.

Huang, W., Wu, X., Hu, L., Wang, L., Ding, Y., & Qu, Z. (2017). Revisiting the earliest electrophysiological correlate of familiar face recognition. *International Journal of Psychophysiology, 120*, 42–53.

Jemel, B., Pisani, M., Calabria, M., Crommelinck, M., & Bruyer, R. (2003). Is the N170 for faces cognitively penetrable? Evidence from repetition priming of mooney faces of familiar and unfamiliar persons. *Cognitive Brain Research, 17*, 431–446.

Jemel, B., Pisani, M., Rousselle, L., Crommelinck, M., & Bruyer, R. (2005). Exploring the functional architecture of person recognition system with event-related potentials in within- and cross-domain priming of faces. *Neuropsychologia, 43*, 2024–2040.

Jemel, B., Schuller, A. M., & Goffaux, V. (2010). Characterizing the spatio-temporal dynamics of the neural events occurring prior to and up to overt recognition of famous faces. *Journal of Cognitive Neuroscience, 22*(10), 2289–2305.

Jenkins, R., White, D., Van Montfort, X., & Burton, A. M. (2011). Variability in photos of the same face. *Cognition, 121*(3), 313–323.

Johnston, R. A., & Edmonds, A. J. (2009). Familiar and unfamiliar face recognition: A review. *Memory, 17*(5), 577–596.

Jonas, J., Jacques, C., Liu-Shuang, J., Brissart, H., Colnat-Coulbois, S., Maillard, L., & Rossion, B. (2016). A face-selective ventral occipito-temporal map of the human brain with intracerebral potentials. *Proceedings of the National Academy of Sciences, 113*(28), E4088–E4097.

Kloth, N., Dobel, C., Schweinberger, S. R., Zwitserlood, P., Bölte, J., & Junghöfer, M. (2006). Effects of personal familiarity on early neuromagnetic correlates of face perception. *European Journal of Neuroscience, 24*(11), 3317–3321.

Lambon Ralph, M. A., Ehsan, S., Baker, G. A., & Rogers, T. T. (2012). Semantic memory is impaired in patients with unilateral anterior temporal lobe resection for temporal lobe epilepsy. *Brain, 135*(1), 242–258.

Leveroni, C. L., Seidenberg, M., Mayer, A. R., Mead, L. A., Binder, J. R., & Rao, S. M. (2000). Neural systems underlying the recognition of familiar and newly learned faces. *Journal of Neuroscience, 20*(2), 878–886.

Liu-Shuang, J., Norcia, A. M., & Rossion, B. (2014). An objective index of individual face discrimination in the right occipito-temporal cortex by means of fast periodic oddball stimulation. *Neuropsychologia, 52*, 57–72.

Liu-Shuang, J., Torfs, K., & Rossion, B. (2016). An objective electrophysiological marker of face individualisation impairment in acquired prosopagnosia with fast periodic visual stimulation. *Neuropsychologia, 83*, 100–113.

Longmore, C. A., Liu, C. H., & Young, A. W. (2008). Learning faces from photographs. *Journal of Experimental Psychology: Human Perception and Performance, 34*(1), 77–100.
Lui, M., Lui, K. F., Wong, A. C. N., & Rosenfeld, J. P. (2018). Suppression of 12-hz SSVEPs when viewing familiar faces: An electrophysiological index to detect recognition. *International Journal of Psychophysiology, 133*, 159–168.
Maris, E., & Oostenveld, R. (2007). Nonparametric statistical testing of EEG-and MEG-data. *Journal of Neuroscience Methods, 164*(1), 177–190.
Megreya, A. M., & Burton, A. M. (2006). Unfamiliar faces are not faces: Evidence from a matching task. *Memory & Cognition, 34*(4), 865–876.
Natu, V., & O'Toole, A. J. (2011). The neural processing of familiar and unfamiliar faces: A review and synopsis. *British Journal of Psychology, 102*(4), 726–747.
Norcia, A. M., Appelbaum, L. G., Ales, J. M., Cottereau, B. R., & Rossion, B. (2015). The steady-state visual evoked potential in vision research: A review. *Journal of Vision, 15*(6), 1–46.
Pierce, K., Haist, F., Sedaghat, F., & Courchesne, E. (2004). The brain response to personally familiar faces in autism: Findings of fusiform activity and beyond. *Brain, 127*(12), 2703–2716.
Pierce, L. J., Scott, L., Boddington, S., Droucker, D., Curran, T., & Tanaka, J. (2011). The n250 brain potential to personally familiar and newly learned faces and objects. *Frontiers in Human Neuroscience, 5*, 111.
Ramon, M. (2015a). Perception of global facial geometry is modulated through experience. *PeerJ, 3*, Article e850.
Ramon, M. (2015b). Differential processing of vertical interfeature relations due to real-life experience with personally familiar faces. *Perception, 44*(4), 368–382.
Ramon, M., & Van Belle, G. (2016). Real-life experience with personally familiar faces enhances discrimination based on global information. *PeerJ, 4*, e1465.
Regan, D. (1966). Some characteristics of average steady-state and transient responses evoked by modulated light. *Electroencephalography and Clinical Neurophysiology, 20*(3), 238–248.
Retter, T. L., Jiang, F., Webster, M. A., & Rossion, B. (2018). Dissociable effects of inter-stimulus interval and presentation duration on rapid face categorization. *Vision Research, 145*, 11–20.
Retter, T. L., & Rossion, B. (2016). Uncovering the neural magnitude and spatio-temporal dynamics of natural image categorization in a fast visual stream. *Neuropsychologia, 91*, 9–28.
Rice, G. E., Hoffman, P., & Ralph, M. A. L. (2015). Graded specialization within and between the anterior temporal lobes. *Annals of the New York Academy of Sciences, 1359*(1), 84–97.
Ritchie, K. L., Smith, F. G., Jenkins, R., Bindemann, M., White, D., & Burton, A. M. (2015b). Viewers base estimates of face matching accuracy on their own familiarity: Explaining the photo-ID paradox. *Cognition, 141*, 161–169.
Rossion, B. (2018). Humans are visual experts at unfamiliar face recognition. *Trends in Cognitive Science, 22*, 471–472.
Rossion, B., Campanella, S., Gomez, C. M., Delinte, A., Debatisse, D., Liard, L., & Guerit, J. M. (1999). Task modulation of brain activity related to familiar and unfamiliar face processing: An ERP study. *Clinical Neurophysiology, 110*(3), 449–462.
Rossion, B., & Jacques, C. (2011). The N170: Understanding the time-course of face perception in the human brain. In S. J. Luck, & E. S. Kappenman (Eds.), *The Oxford handbook of event-related potential components* (pp. 115–142). New York: Oxford University Press.
Rossion, B., Jacques, C., & Jonas, J. (2018). Mapping face categorization in the human ventral occipitotemporal cortex with direct neural intracranial recordings. *Annals of the New York Academy of Sciences, 1426*(1), 5–24.
Rossion, B., Retter, T., & Liu-Shuang, J. (2020). Understanding human individuation of unfamiliar faces with oddball fast periodic visual stimulation and electroencephalography. *European Journal of Neuroscience* (in press).
Rossion, B., Schiltz, C., & Crommelinck, M. (2003). The functionally defined right occipital and fusiform "face areas" discriminate novel from visually familiar faces. *Neuroimage, 19*(3), 877–883.
Schwartz, L., & Yovel, G. (2016). The roles of perceptual and conceptual information in face recognition. *Journal of Experimental Psychology: General, 145*(11), 1493–1511.
Schweinberger, S. R., Huddy, V., & Burton, A. M. (2004). N250r: A face-selective brain response to stimulus repetitions. *Neuroreport, 15*(9), 1501–1505.
Schweinberger, S. R., Pickering, E. C., Jentzsch, I., Burton, A. M., & Kaufmann, J. M. (2002). Event-related brain potential evidence for a response of inferior temporal cortex to familiar face repetitions. *Cognitive Brain Research, 14*, 398–409.
Sergent, J., Ohta, S., & MacDonald, B. (1992). Functional neuroanatomy of face and object process- ing. A positron emission tomography study. *Brain, 115*, 15–36.
Tanaka, J. W., Curran, T., Porterfield, A. L., & Collins, D. (2006). Activation of preexisting and acquired face representations: The N250 event-related potential as an index of face familiarity. *Journal of Cognitive Neuroscience, 18*(9), 1488–1497.
Todd, R. M., Lewis, M. D., Meusel, L. A., & Zelazo, P. D. (2008). The time course of social-emotional processing in early childhood: ERP responses to facial affect and personal familiarity in a go-nogo task. *Neuropsychologia, 46*(2), 595–613.
Volfart, A., Jonas, J., Maillard, L., Colnat-Coulbois, S., & Rossion, B. (2020). Neurophysiological evidence for crossmodal (face-name) person-identity representation in the human left ventral temporal cortex. *PLoS Biology, 18*(4), Article e3000659.
Wandell, B. A. (2011). The neurobiological basis of seeing words. *Annals of the New York Academy of Science, 1224*(1), 63–80.
Wiese, H., Tüttenberg, S. C., Ingram, B. T., Chan, C. Y., Gurbuz, Z., Burton, A. M., & Young, A. W. (2019). A robust neural index of high face familiarity. *Psychological Science, 30*(2), 261–272.
Wild-Wall, N., Dimigen, O., & Sommer, W. (2008). Interaction of facial expressions and familiarity: ERP evidence. *Biological Psychology, 77*, 138–149.
Yan, X., Liu-Shuang, J., & Rossion, B. (2019). Effect of face-related task on rapid individual face discrimination. *Neuropsychologia, 129*, 236–245.
Yan, X., Zimmermann, F. G., & Rossion, B. (2020). An implicit neural familiar face identity recognition response across widely variable natural views in the human brain. *Cognitive Neuroscience, 11*(3), 143–156.
Young, A. W., & Burton, A. M. (2018). Are we face experts? *Trends in Cognitive Sciences, 22*(2), 100–110.
Zimmermann, F. G., Yan, X., & Rossion, B. (2019). An objective, sensitive and ecologically valid neural measure of rapid human individual face recognition. *Royal Society Open Science, 6*(6), 181904.